Concurrent Dual-Band GaN-HEMT Power Amplifier at 1.8 GHz and 2.4 GHz

[#1]Paul Saad, [*2]Paolo Colantonio, [†]Junghwan Moon, [*]Luca Piazzon, [*]Franco Giannini,
[#]Kristoffer Andersson,[†]Bumman Kim, and [#]Christian Fager
[#]Department of Microtechnology and Nanoscience, Chalmers University of Technology, Gothenburg, Sweden
e-mail: [1]paul.saad@chalmers.se
[*]Department of Electronic Engineering, University of Rome Tor Vergata, Rome, Italy
e-mail: [2]paolo.colantonio@uniroma2.it
[†]Department of Electrical Engineering, Pohang University of Science and Technology, Pohang, South Korea

***Abstract*—This paper presents the design, implementation, and experimental results of a highly efficient concurrent dual-band GaN-HEMT power amplifier at 1.8 GHz and 2.4 GHz. A bare-die approach, in conjunction with a harmonic source-pull/load-pull simulation approach, are used in order to design and implement the harmonically tuned dual-band PA.**
For a continuous wave output power of 42.3 dBm the measured gain is 12 dB in the two frequency bands; while the power added efficiency is 64% in both bands. Linearized modulated measurements, using concurrently 10MHz LTE and WiMAX signals, show an average PAE of 25% and and adjacent channel leakage ratio of -48 dBc and -47 dBc at 1.8 GHz and 2.4 GHz, respectively.

Keywords- power amplifier (PA); dual-band, gallium nitride (GaN); high electron mobility transistor (HEMT); harmonic termination, digital predistortion (DPD)

I. INTRODUCTION

The fast evolution of wireless communication systems and the roll-out of new communication standards increase the need for multi-band transceivers that can manage simultaneously different standards [1].
Software Defined Radio is recently introduced to implement wireless radios capable of dealing with these requirements through software reprogramming [2]. However, the major issues reside in the RF front-end stage that requires the development of multi-band/multi-standard circuits and subsystems. A critical component for multi-band or multi-standard operation is the power amplifier (PA). In fact, it should simultaneously satisfy low-distortion and high-efficiency requirements, accounting for the amplifying signal features in terms of amplitude variation and bandwidth [3]-[5].
Successful design methodology for the design of single-band high efficiency microwave PAs has been presented in [6]-[7]. In this paper, the capabilities of this methodology for dual-band applications are explored.This is demonstrated by the design of a dual-band harmonically tuned GaN-HEMT PA at 1.8 GHz and 2.4 GHz.
This paper is organized as follows. In Sec. II, a description of the design approach and the implementation of the dual-band PA is presented. The experimental results are presented in Sec. III, while conclusions are given in Sec. IV.

II. DUAL-BAND PA DESIGN AND IMPLEMENTATION

In the design, the 3.6 mm GaN bare-die device, Cree CGH60015DE, has been used. The device has a breakdown voltage of 100V, a pinch-off voltage of -3.2 V, and a saturation drain current of 2.3 A, approximately. An optimized Class-AB nonlinear model ofthe device, supplied by the manufacturer, has been used for the design.
The parasitics deteriorate the PA performance. By using a bare-die mounting approach, the most important parasitics associated with the package, such as the lead inductances and tab capacitances, have been minimized. The bare-die transistor chip is mounted to the PA fixture and connected directly to the printed circuit boards (PCBs) using wire bonding. The chip and PCB surfaces have been carefully aligned to minimize the bond wire lengths.
The first step to design the PA was to perform load-pull/source-pull simulations, at 1.8 GHz and 2.4 GHz, at the die reference plane in order to find the fundamental load and source impedances that maximize the output power of the PA. The obtained optimum fundamental impedances were used to perform harmonic load-pull simulations to study the effect of the harmonics on the efficiency performance.

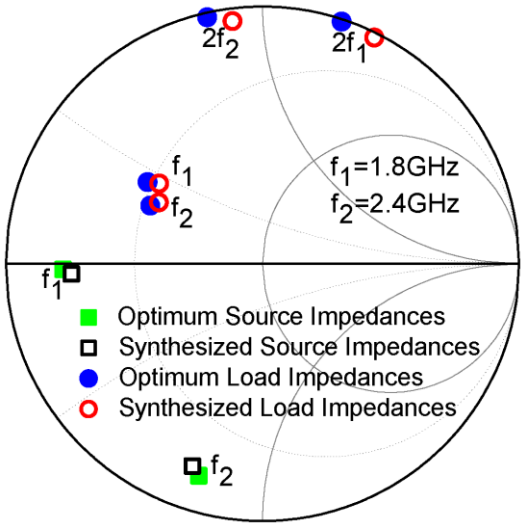

Figure 1.Simulated optimum impedances, at the transistor reference plane for maximum output power.

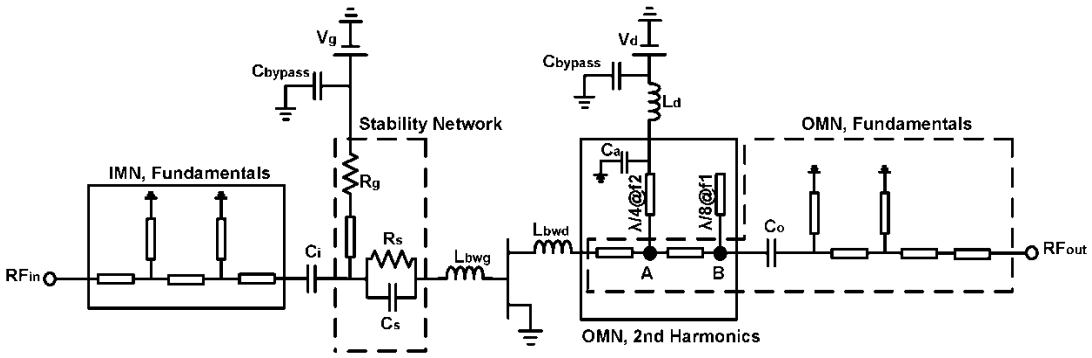

Figure 2.Circuit diagram of the dual-band PA.

The simulations verified that terminations of the second harmonic at the input and the third harmonic at the output have negligible impact on the efficiency. Consequently, to reduce the complexity of the matching networks, such harmonics have been neglected in the design of the respective network. The resulting optimum source and load impedances at fundamentals that maximize the output power and the load impedances at the second harmonic that maximize the PAE are shown in Fig. 1. The filled symbols are the loads identified by load-pull/source-pull simulations, while the empty symbols are the final impedances synthesized by a distributed approach [8].

The circuit diagram of the designed dual-band PA is shown in Fig. 2. The inductances L_{bwg} and L_{bwd} are used in the circuit design to model the input and output bond-wire inductances, respectively. Their estimated values are 0.15 nH each.

The output matching network consists of two sub-networks, used to control the 2nd harmonic loading conditions (the distributed network surrounded by the solid rectangle in Fig. 2) and the two fundamental impedances (dashed rectangle). For the harmonics, the parallel quarter-wave TL at f_2, shorted by the C_a capacitor, provides a short circuit for the second harmonic of f_2 at node A. Similarly, the parallel eighth-wave at f_1 open-circuited stub provides a short circuit forth second harmonic of f_1 at node B. The matching at the two fundamental frequencies, f_1 and f_2, is provided by the remaining TLs and short-circuited stubs.

The input matching network consists of the distributed network surrounded by the solid rectangle that provides the input matching simultaneously at the two fundamental frequencies f_1 and f_2. The network surrounded by dashed box, is a stabilization network that provides the stability of the dual-band PA in-band and at low frequencies. This network was included in the load-pull/source-pull simulations. Monte-Carlo (MC) and Electromagnetic (EM) simulations were performed to study the reliability and the robustness of the designed dual-band PA. EM simulations were performed on the transmission line parts of the input and output matching networks. MC simulations studied the uncertainties introduced by the lumped components and the manufacturing process. The EM and MC simulations have shown that the design is robust, not very sensitive to these effects and therefore no tuning or modifications were required.

The dual-band PA was implemented on a Rogers 5870 substrate with ε_r = 2.33 and thickness of 0.8 mm. To facilitate wire bonding the PCBs were gold plated. Fig. 3 shows a picture of the implemented dual-band PA using the bare-die GaN-HEMT device. The bare-die device was attached to the aluminum fixture ridge. From each side of the ridge, the input and output PCBs were attached separately and connected to the device using three bond wires from each side. Moreover, no post-production tuning was used after the implementation of the PA.

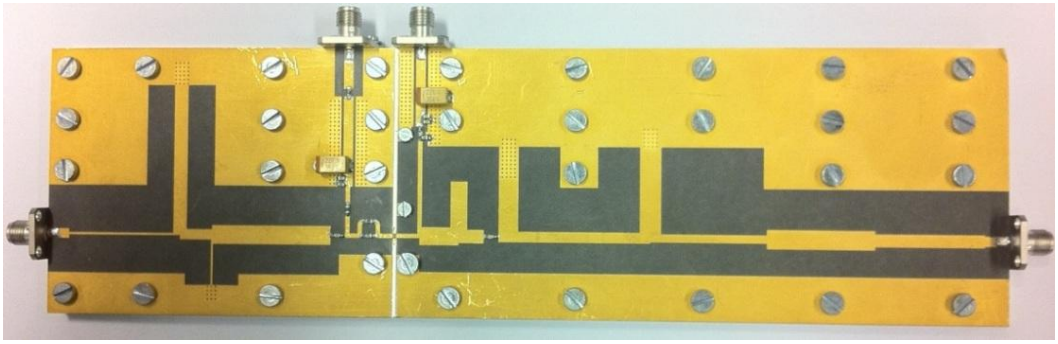

Figure 3. Photo of the implemented dual-band PA, size = 6 × 20 cm^2.

III. Measurement Results

The implemented PA has been characterized by small-signal, large-signal and modulated-signals measurements to verify its performance.

A. Smal-Signal Measurements

The scattering-parameters of the realized dual-band PA were measured using Agilent E8361A PNA. A drain bias of V_{DD} = 30 V, and a quiescent drain current of 150 mA (gate voltage of −3 V) were used for this measurement. The measured S-parameters, presented in Fig. 4, show a very good agreement with simulations and therefore, it demonstrates the correct behavior of the PA in the proximity of 1.8 GHz and 2.4 GHz. The input match (S11) is better than 20 dB at 1.8 GHz and better than 13 dB at 2.4 GHz while the output match (S22) is better than 15 dB at both bands. The small-signal gain (S21) is around 16 dB in the two bands.

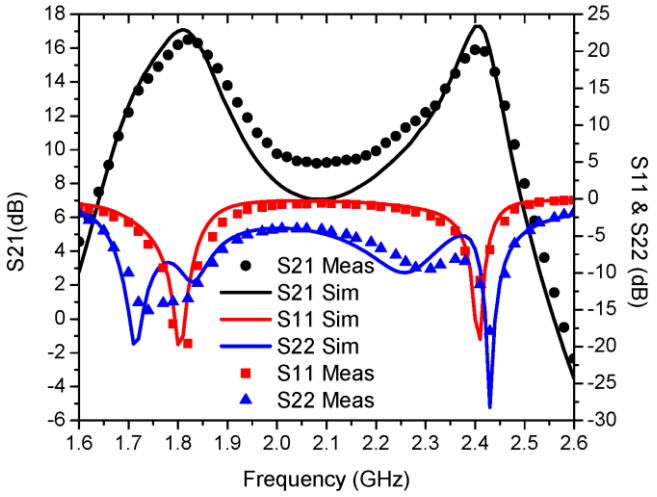

Figure 4.Measured and simulated S-parameters of the dual-band PA.

B. Large-Signal Measurements

Continuous wave (CW) input signals have been generated by a microwave synthesized source (Agilent E4438C) boosted by a microwave driver amplifier and the output power levels were measured by a power meter (Agilent E4419B). The chosen dc bias is the same as for the S-parameter measurement.

The dual-band PA has been characterized versus frequency between 1.6 GHz and 2.6 GHz, with a 30 dBm fixed input power drive level.

From Fig. 5, it can be noted that the agreement between simulations and measurements is very good and the center frequency is accurately predicted by the simulations. The measured peak PAE is 64% in the two bands, with a measured output power of 42.3 dBm at 1.8 GHz and 42 dBm at 2.4 GHz.

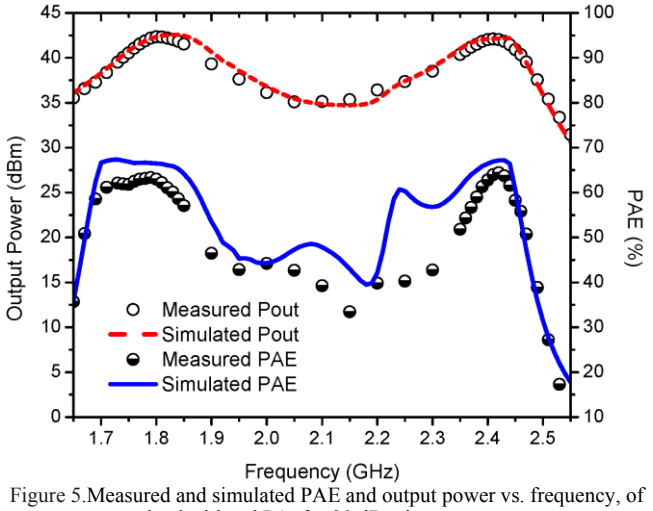

Figure 5.Measured and simulated PAE and output power vs. frequency, of the dual-band PA, for 30 dBm input power.

The amplifier exhibits a PAE higher than 50% between 1.67 GHz and 1.87 GHz and between 2.34 GHz and 2.48 GHz. This corresponds to 11% and 6% fractional bandwidth around 1.8 GHz and 2.4 GHz bands, respectively.

Fig. 6 shows measured power gain and PAE versus input power at 1.8 GHz and 2.4 GHz, respectively. It can be noticed the performance and behavior of the PA are the same in the two operating bands. For 3-dB gain compression, corresponding to 30 dBm input power; the measured PAE is 64% in both bands, while the measured gain is 12.3 dB at 1.8 GHz and 12 dB at 2.4 GHz.

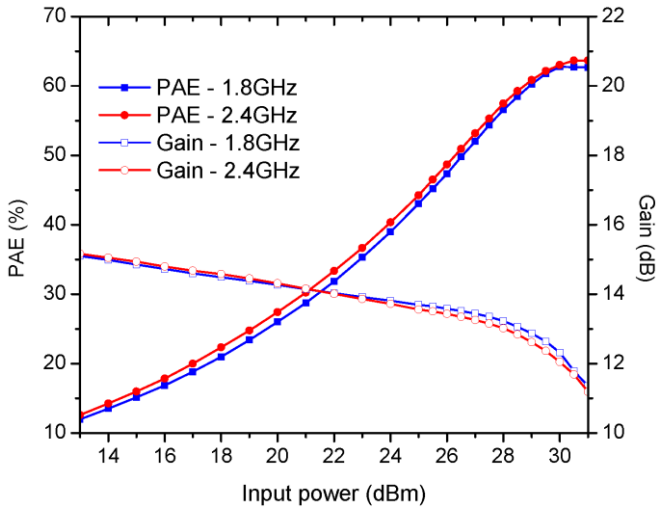

Figure 6.Measured PAE and power gain vs. input power, of the dual-band PA, at 1.8GHz and 2.4GHz.

C. Modulated Measurements

To demonstrate that the dual-band PA is linearizable and able to meet modern wireless communication system standards, modulated measurements have been performed. The digital-predistortion (DPD) used, is the memory polynomial model with nonlinear 7 and memory depth 3 [9]. The PA has been tested first using one modulated signal

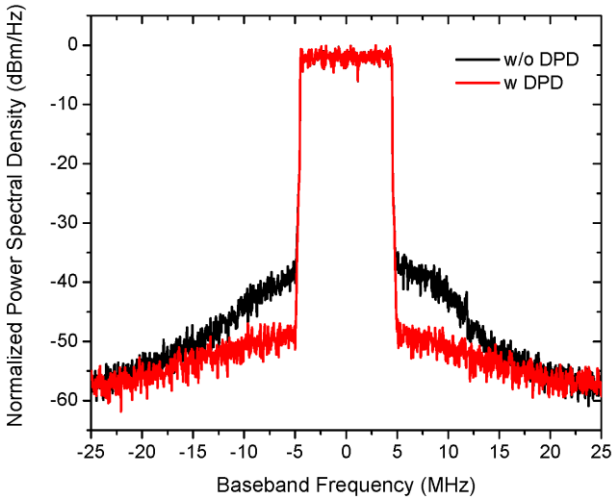

Figure 7. PA output signal spectrum of a 10 MHz LTE signal at center frequency of 1.8 GHz before and after digital-predistortion.

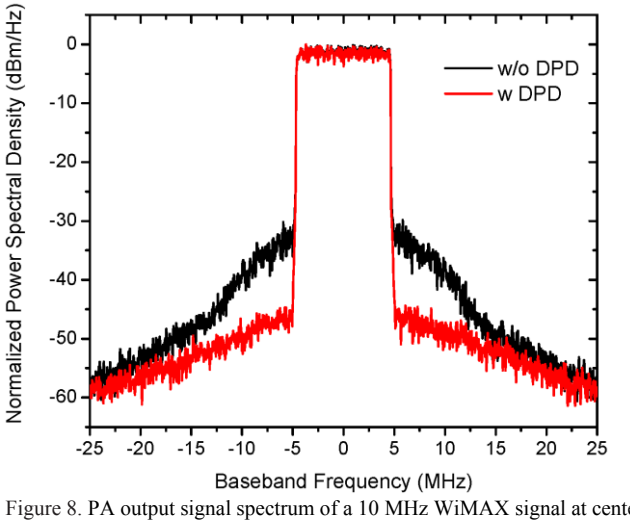

Figure 8. PA output signal spectrum of a 10 MHz WiMAX signal at center frequency of 1.8 GHz before and after digital-predistortion.

(non-concurrent mode). The signals used are 5 MHz WCDMA, 10 MHz LTE signals both with 7 dB Peak-to-Average-Ratio (PAR), and WiMAX signal with 8.5 dB PAR. Average output power, PAE, and ACLR, with and without DPD are summarized in Table I.

Table I. AVERAGE POUT, AVERAGE PAE, AND ACLR.

	Pout (dBm)		PAE (%)		ACLR (dBc)	
	w/o DPD	w DPD	w/o DPD	w DPD	w/o DPD	w DPD
WCDMA @ 1.8GHz	35.5	35.4	34.7	34.5	-36.6	-53.1
WiMax @ 2.4GHz	34.5	34.7	29.9	30.3	-37.4	-51.7
LTE @ 1.8GHz	35.5	35.6	34.6	35.5	-35.2	-52.6
LTE @ 2.4GHz	35.5	35.5	32.7	33.3	-33.3	-49

Then the PA has been tested in concurrent mode. The linearization was performed with the 2-D-DPD technique presented in [10].

In the first experiment, the WCDMA and the LTE signal were used at 1.8 GHz and 2.4 GHz bands respectively. In the second experiment the LTE signal is used at 1.8 GHz band while the WiMAX signal is used at the 2.4 GHz band.

The measured output spectrum at 1.8 GHz and 2.4 GHz (second experiment), before and after DPD, for an average input power of 19 dBm, are shown in Fig. 7 and Fig. 8, respectively. Average output power, PAE, and ACLR, with and without DPD of the two experiments, at the two operating bands, are summarized in Table II. We notice that the average PAE is degraded by 5-10% compared to the case where the PA is driven by one modulated signal at the time (Table I).

Table II. AVERAGE POUT, AVERAGE PAE, AND ACLR.

	Pout (dBm)		PAE (%)		ACLR (dBc)	
	w/o DPD	w DPD	w/o DPD	w DPD	w/o DPD	w DPD
WCDMA @ 1.8 GHz	33	33	24.7	25	-36.7	-48.8
LTE @ 2.4 GHz					-37.5	-47.5
LTE @ 1.8 GHz	33	33	24.5	25	-34.3	-47.6
WiMAX @ 2.4 GHz					-39	-46.5

Yet, these results show that standard DPD methods can be used to linearize the DPA in concurrent modes to meet modern wireless communication system standards.

IV. CONCLUSION

In this paper, the design of a concurrent dual-band high efficiency harmonically tuned PA using a GaN-HEMT has been presented. Using bare-die devices and the design approach based on harmonic load-pull/source-pull simulations have allowed the realization of high performance dual-band PA at 1.8 GHz and 2.4 GHz. The CW measurement showed, in both bands, a power gain of 12 dB, peak PAE of 64% and an output power of 42.3 dBm. An average PAE of 25% was recorded when LTE and WiMAX signals were applied concurrently.

ACKNOWLEDGMENT

This research has been carried out in the University of Roma Tor Vergata and in the GigaHertz Centre in a joint project financed by the Swedish Governmental Agency for Innovation Systems(VINNOVA), Chalmers University of Technology, ComHeat Microwave AB, Ericsson AB, Infineon Technologies Austria AG, Mitsubishi Electric

Corporation, NXP Semiconductors BV, Saab AB, and SP Technical Research Institute of Sweden.

REFERENCES

[1] J.-M. Chung, K. Park, T. Won, W. Oh, and S. Choi, "New protocol for future wireless systems," in 53rd IEEE Int. Midwest Symp. Circuits Syst., Aug. 2010, pp. 692–695.

[2] H. Arslan, Cognitive Radio, Software Defined Radio, and AdaptiveWireless Systems. Springer, 2007.

[3] A. Grebennikov and N. Sokal, "Switchmode RF power Amplifiers," Newnes, 2007.

[4] S. C. Cripps, "RF Power Amplifiers for Wireless Communications," Norwood, MA: Artech House, 2006.

[5] P. Colantonio, F. Giannini, and E. Limiti, High Efficiency RF and Microwave Solid State Power Amplifiers. John Wiley & Sons, 2009.

[6] P. Saad, C. Fager, H. Nemati, H. Cao, H. Zirath, and K. Andersson, "A Highly Efficient 3.5 GHz Inverse Class-F GaN HEMT Power Amplifier," in International Journal of Microwave and Wireless technologies, vol. 2, no. 3-4, pp. 317– 324, Aug. 2010.

[7] P. Saad, H. Nemati, K. Andersson, and C. Fager, "Highly efficient GaN-HEMT power amplifiers at 3.5 GHz and 5.5 GHz," in Wireless and Microwave Technology Conference (WAMICON), Apr. 2011.

[8] P. Colantonio, F. Giannini, R. Giofrè, and L. Piazzon, "A design technique for concurrent dual band harmonic tuned power amplifier," IEEE Trans. Microw. Theory Tech., vol. 56, no. 11-II, pp. 2545-2555, Nov. 2008.

[9] J. Kim and K. Konstantinou, "Digital predistortion of wideband signals based on power amplifier model with memory," *Electron. Lett.*, vol. 37, no. 23, pp. 1417–1418, Nov 2001.

[10] W. Chen, S. A. Bassam, X. Li, Y. Liu, K. Rawat, M. Helaoui, F. M. Ghannouchi, and Z. Feng, "Design and linearization of concurrent dualband doherty power amplifier with frequency-dependent power ranges,"*IEEE Trans.* vol. 59, no. 10, pp. 2537-2546,Oct. 2011.